

# Flow over a Twin-Tailed Aircraft at Angle of Attack, Part II: Temporal Characteristics

N. M. Komerath,\* R. J. Schwartz,† and J. M. Kim†  
Georgia Institute of Technology, Atlanta, Georgia 30332

Aircraft with twin vertical tails have encountered buffeting problems at high angles of attack. This paper presents the second part of an effort to define the aerodynamic environment of the vertical tails at high angles of attack. Previous measurements of the time-averaged flowfield are extended here to study the spectral content of the fluctuations in the vicinity of the vertical tails using hot-film anemometry. Sharply peaked spectra are observed both inboard and outboard of the upper portion of the vertical tails. A high-frequency hump is seen in the spectra obtained upstream of the wing roots and between the vertical tails. Broadband turbulent spectra are observed elsewhere. The narrow-band fluctuations appear to originate in the separated flow over the wing surfaces. Comparison of velocity spectra from models of different sizes, at different freestream velocities, demonstrates scaling of the dominant spectral peak with Strouhal number over a wide range of Reynolds number, Mach number, and dynamic pressure. The Strouhal number also matches that of the peak of the acceleration spectrum on the vertical tail of a full-scale F-15 at Mach 0.6. This, coupled with previous wind-tunnel tests on rigid and aeroelastically scaled models, demonstrates that the tail oscillations are driven by narrow-band fluid-dynamic oscillations, whose frequency varies with angle of attack and flight velocity. Thus, narrow-band velocity fluctuations occur in the high- $\alpha$  flowfield even in the absence of strong vortices.

## Nomenclature

$c_{av}$	= mean geometric chord
$f$	= frequency in cycles per second
$S$	= wing span
$U_{\infty}$	= freestream velocity
$V_{rms}$	= root-mean-square velocity fluctuation sensed by single hot film
$\alpha$	= aircraft angle of attack
$\Delta f$	= frequency resolution of spectral analysis
$\Lambda$	= wing leading-edge sweep
$\lambda$	= wing taper ratio

## Introduction

THIS paper studies the fluctuations present in the flowfield over twin-tailed swept-wing aircraft at high angles of attack. The severe buffeting experienced by control surfaces immersed in such flows has become a matter of interest from considerations of aerodynamic stability and structural fatigue. Reference 1 presents the first part of this work, and discusses other recent related work. The time-averaged velocity field of the F-15 has been related to laser sheet visualization of the vortical flow patterns and trajectories and tuft visualization of flow separation. Vorticity contours were used to examine the flow in cross-flow planes over the inlet, the wing, and upstream of the vertical tails. The flow angularity at the vertical tails was seen to depend strongly on  $\alpha$ . The angularity varied from the root to the tip of the tail and fluctuated over a wide range.

Reference 2 reported surface pressure measurements on rigid and aeroelastically scaled vertical tails. Here, the spectra showed broad-band humps. The root-mean-square levels on the inside surfaces were substantially lower than those on the outboard surfaces for the rigid tail. Fluctuating loads on the elastic tails were substantially (25%) higher than those on the rigid tails, and the root-mean-square levels on the elastic tails were of the same order both inboard and outboard. Sharp

spectral peaks occurred at the frequencies of structural modes of the elastic tails. Reference 3 reported predominant peaks in the spectra of velocity fluctuations upstream of the F-15 vertical tails. The peak frequencies varied with angle of attack, dynamic pressure, and location. Spectra were not explicitly shown.

Past work leads to two different hypotheses, in the present authors' opinion, about the nature of the tail vibrations. These are illustrated in Fig. 1. The broad-band pressure spectra of Ref. 2 may be used to conclude that the structure responds at its critical frequencies to a broadband excitation, in a highly turbulent flow. This is hypothesis I. On the other hand, the velocity data of Ref. 3 and some of the sharp-peaked spectra in Ref. 2 lead one to suspect that the structure is driven by quasiperiodic flow fluctuations. This can occur even in a flow where the turbulent intensity is quite low. At some flight conditions, the structural modes of the tails coincide with the dominant frequency of the flow fluctuations. This is hypothesis II. These two hypotheses have quite different implications for the computation of the environment, and perhaps for the design of the tails.

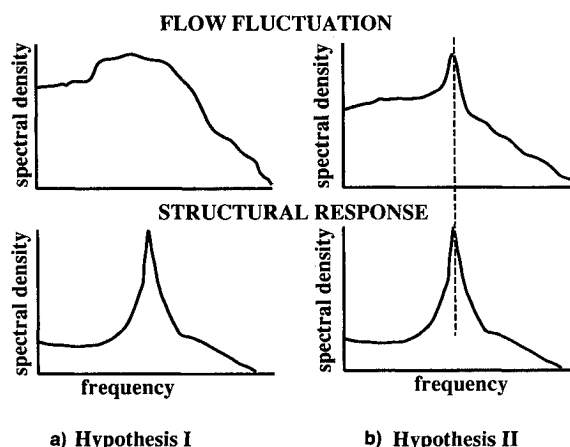


Fig. 1 Hypotheses regarding the mechanism of fin buffeting, based on previous F-15 work.

Received Oct. 31, 1990; revision received May 22, 1991; accepted for publication May 23, 1991. Copyright © 1991 by the American Institute of Aeronautics and Astronautics, Inc. All rights reserved.

\*Associate Professor, School of Aerospace Engineering.

†Graduate Research Assistant, School of Aerospace Engineering.

### Present Scope and Objectives

The present objective is to study the frequency content in the velocity field around a widely used twin-tailed aircraft, the F-15 at high angles of attack. This is to aid in developing analytical models of the velocity fluctuations, in turn to assist the development of computational methods for prediction of tail buffeting phenomena. The dependence of these frequencies on angle of attack and freestream velocity are examined. Data from models of different sizes are correlated, and some flight test results are examined. This work builds on the definition of the spatial variations of the velocity field described in Ref. 1. The flow is incompressible, and the Reynolds number is far below full-scale flight values. The justifications for these<sup>1</sup> will be re-examined by comparing Strouhal numbers over a wide range of Reynolds number and Mach number.

### Experimental Technique

The experiments were conducted in the John J. Harper Low-Speed Wind Tunnel. Turbulence intensity is less than 0.5% over the speed range of interest. In addition to the  $\frac{1}{8}$ -scale stiffened plastic models,<sup>1</sup> a  $\frac{1}{4}$ -scale model was assembled from a fiberglass kit, stiffened, and mounted on a 3-point system, with one telescoping support under the forebody and one under each wing. The supports were mounted on rails to enable adjustment of  $\alpha$ . The left wing was instrumented with static pressure taps, and one of the vertical tails was replaced with a tail with scaled airfoil sections. The model was tufted for flow visualization. The horizontal stabilizers were connected to radio-controlled servo motors.

#### Hot-Film Anemometry

A single-sensor hot-film probe was traversed to different stations (Fig. 2) in the flowfield under computer control. The vertical line at station 10 intersects the observed trajectory of the center of the vortex system.<sup>1</sup> Station 12 is directly downstream of station 10. Station 14 is directly upstream of the vertical tail, and station 16 is in the vertical plane of symmetry, midway between the two vertical tails. Station 18 is a line parallel to and just upstream of the vertical tail leading edge. Station 20 is a line through the midchord of the tail, just off the inboard surface, and station 22 is the corresponding line just off the outboard surface at midchord. The anemometer signal was digitized with 16-bit precision through two channels: the first providing the full hot-film signal, and the second being high-pass filtered at 1 Hz and amplified for optimal signal level. Both channels were low-pass filtered at 600 Hz before digitization. The sampling rate was 1400/s, giving a Nyquist frequency of 700 Hz. Each time-domain sample block had 512 samples, producing 256 points in the complex frequency domain. The digitization parameters were arrived at

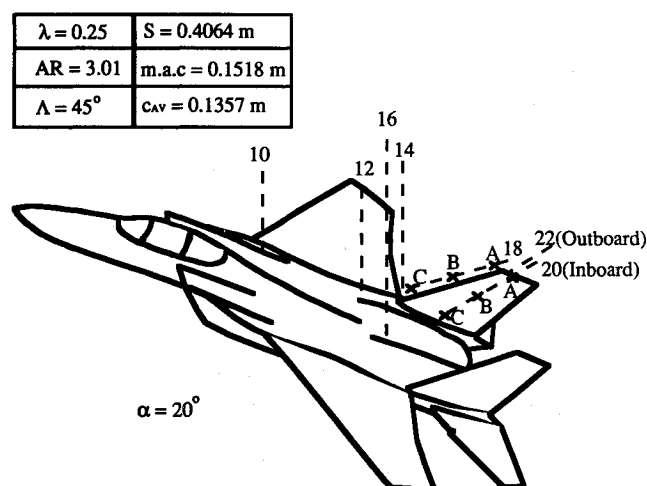


Fig. 2 Hot-film measurement stations above the  $\frac{1}{4}$ -scale model.

by trial and error, with the bandwidth varied at each station to check for other significant phenomena. Each digitized value was converted to velocity using the full nonlinear calibration of the sensor, predetermined using a pitot-static probe. At every measuring point, 100 such sample blocks were used to find stable, averaged auto-spectra of the velocity fluctuations. In the following figures, the spectral density of the velocity fluctuations is in  $(\text{m/s})^2/(\Delta f)$ . For the Nyquist frequency of 700 Hz with 256 frequency intervals as given above,  $\Delta f$  is 2.7344 Hz.

#### Preliminary Checks

It was verified that spectral shapes were not affected by probe orientation. All reported data were taken with the sensor perpendicular to the freestream. The single-sensor hot-film is thus equally sensitive to both vertical and streamwise velocity and less sensitive to lateral velocity. Fluctuations in all three velocity components are significant here, and hence we make no attempt to resolve the fluctuations into individual components. We focus only on the frequency content.

A long, thin probe with a single sensor minimized probe interference. Probe vibration was checked by measuring spectra with various combinations of support stiffness and orientation. Spectral shapes were unchanged in the range of interest. Probe vibration caused a peak at very low frequency and some broadband noise. The rms value did change with some configurations. The configuration with the lowest rms was used.

#### Structural Vibrations

During the initial phase of this program, an unmodified plastic model was used for exploratory velocity measurements. After a few hours at 30.48 m/s at  $\alpha = 20$  deg, one of the vertical tails flew off down the tunnel, and the other went into violent oscillations. Following this incident, the models were greatly strengthened for all data acquisition, including the laser velocimetry in Ref. 1, with the interior hardened with automobile body filler compound, and the wings and tails reinforced with metal plates. A videocamera zoom lens was focused on the vertical tail tips to check for vibrations which would have affected the clarity of the image of the edges. None were found. Further measurements of structural dynamics were not pursued.

### Results

#### Velocity Spectra at $\alpha = 20$ deg

The baseline test condition was at  $\alpha = 20$  deg and  $U_\infty = 30.48 \text{ m/s}$ , with a  $\frac{1}{4}$ -scale model. Figure 3 shows the velocity

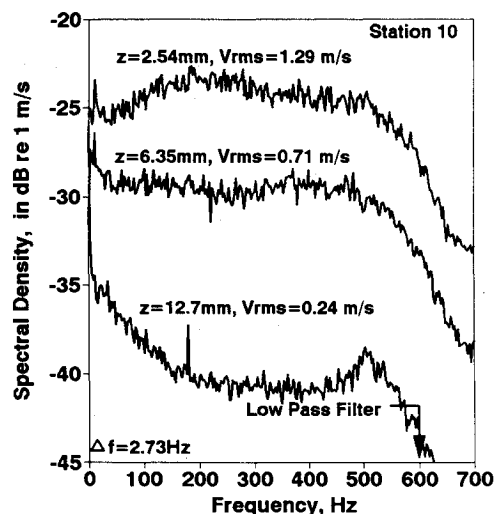


Fig. 3 Hot-film velocity spectra at station 10 at various distances above the surface.

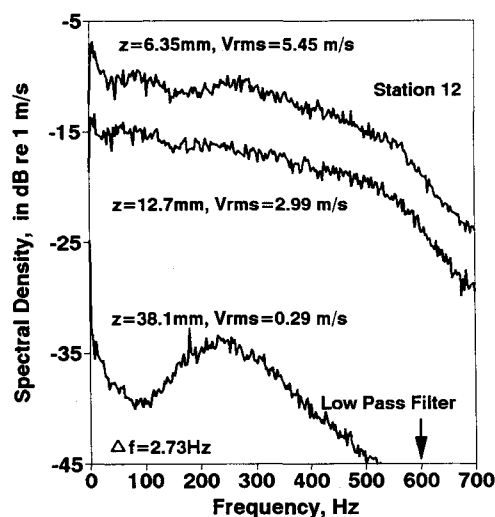


Fig. 4 Hot-film velocity spectrum at station 12 at various distances above the surface.

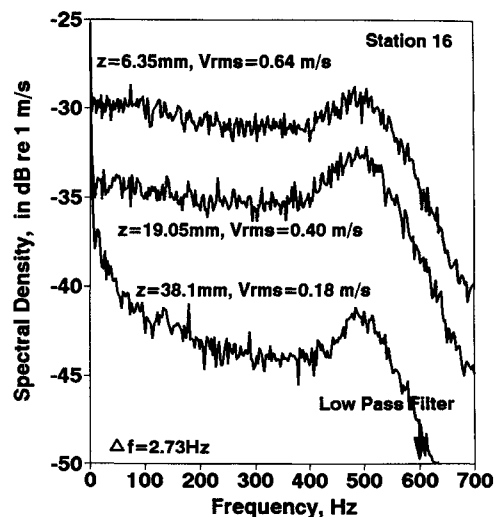


Fig. 6 Hot-film velocity spectrum at station 16 at various distances above the surface.

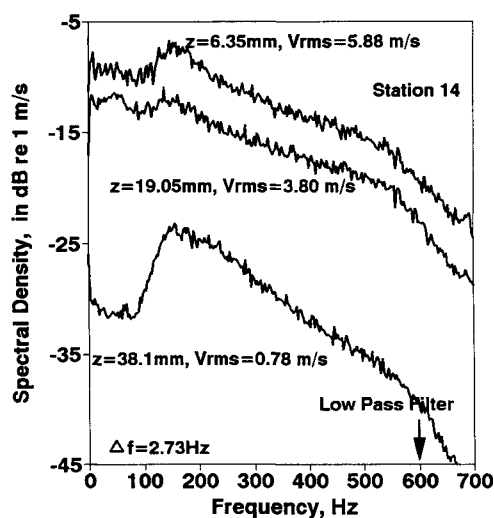
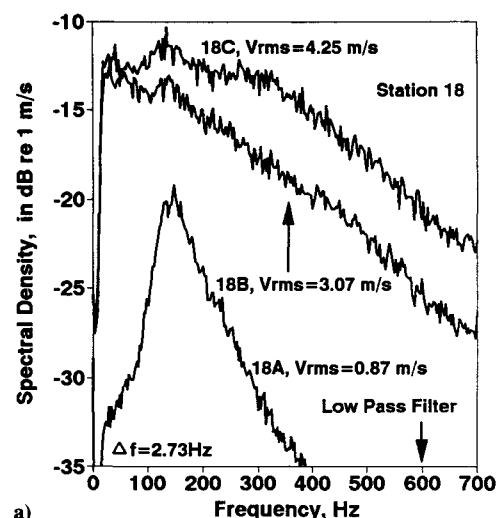


Fig. 5 Hot-film velocity spectrum at station 14 at various distances above the surface.

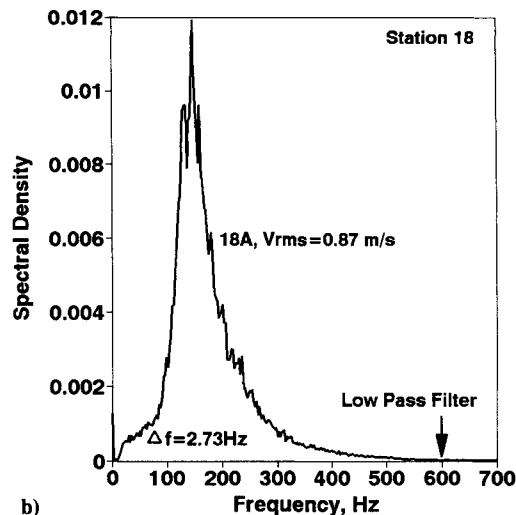
spectra at station 10. The ordinate is in  $10 \cdot \log_{10}(G)$ , where  $G$  is the spectral density. The reference value of velocity fluctuation used is thus 1 m/s. At 2.54 mm above the surface, we see mainly the broadband spectrum of boundary-layer turbulence. The small low-frequency spike is unexplained. A similar spectral shape occurs at 6.35 mm above the surface. At 12.7 mm, the turbulence level is much lower, but a sharp spike occurs at around 180 Hz. There is also a high-frequency hump centered at 500 Hz. By varying Nyquist frequency and low-pass filter settings, we verified that this hump was fully captured. Going downstream, we see again broadband spectra in Fig. 4 at station 12. The 500 Hz rise is absent. At 38.1 mm, where the turbulence is low, the 180 Hz peak is visible, in addition to a broad peak centered around 250 Hz.

At station 14, the spectral content is quite different. Figure 5 shows a peak near 180 Hz at 6.35 and 19.05 mm above the surface, becoming dominant at 38.1 mm above the surface. The spectral energy appears to have been channeled into this narrow band.

Going to the plane of symmetry between the tails, Figure 6 shows the spectra at station 16. The spectrum nearest the surface has significant energy in a hump around 500 Hz. This feature becomes clearer higher above the surface as the turbulence intensity drops. This suggests that the flow structures at station 10 move inboard and downstream between the vertical tails. At large yaw angles, this may cause fluctuating



a)



b)

Fig. 7 a) Velocity spectra at station 18, along the vertical tail leading edge at  $\alpha = 20$  deg; b) spectrum at point 18A, plotted using linear ordinates.

loads at a frequency of about 3 times the dominant frequency seen in the following figures.

Station 18A (Fig. 7a) is upstream of and close to the top of the vertical tail leading edge. The spectrum at this location is replotted in Fig. 7b using a linear ordinate to show the

existence of a very sharp, dominant spectral peak at 150 Hz. This indicates a periodic or quasiperiodic fluctuation. The peak appears to be an amplified version of the feature appearing at station 14 (Fig. 5). The frequency band is narrower by about 50%, and the spectral density exceeds twice that of the peak at station 14. Roughly 80% of the fluctuation energy is concentrated within this narrow band. Station 18B is close to the leading edge of the vertical tail, but at midspan. The turbulence intensity is much higher than at station 18A. The 150-Hz peak is almost lost in the broadband turbulence. At station 18C, the 150-Hz peak is present but not dominant. High-intensity turbulence is seen.

Figure 8 shows spectra measured close to the inboard surface of the vertical tail, at midchord of the tail. The narrow 150-Hz peak is dominant at stations 20A and 20B but is absent in the broad spectrum at station 20C, near the root of the tail. Turbulence intensity is also low. This may be due to the constraint imposed by the "channel flow" between the tails. Figure 9 shows spectra at corresponding positions outboard of the vertical tail, again along the midchord line. Now the narrowband peak is present only at station 22A, near the top of the tail, and not even at station 22B. Again, as observed in the tuft studies of Ref. 1, the intensity of fluctuations near the outboard surface of the vertical tails is much higher than that near the inboard surface.

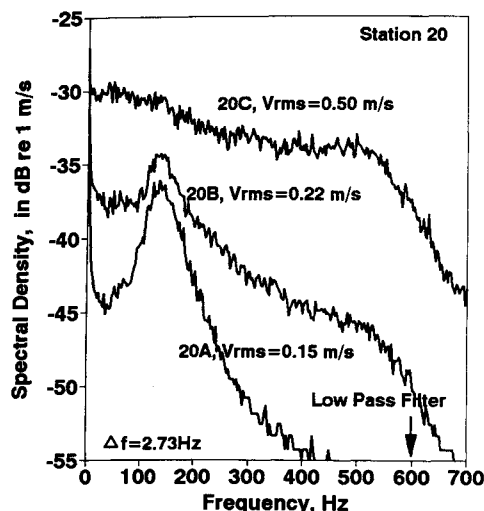


Fig. 8 Velocity spectra at station 20, close to the inboard surface at mid-chord.

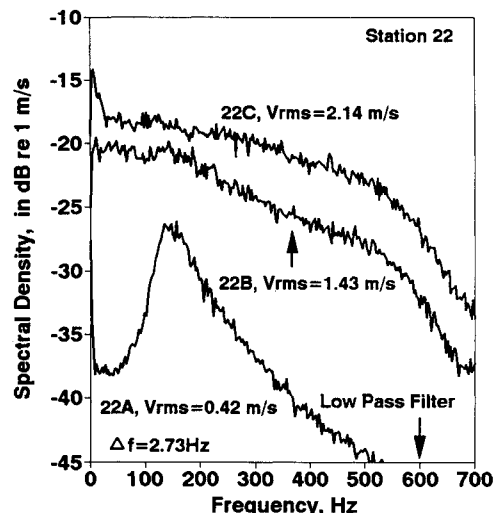


Fig. 9 Velocity spectra at station 22, close to the outboard surface at mid-chord.

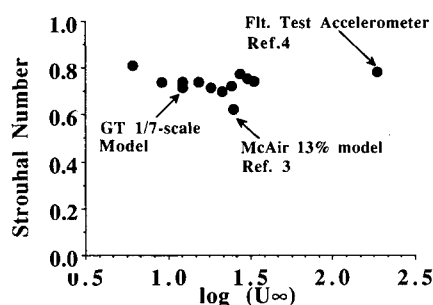


Fig. 10 Summary of the data from hot-film anemometry and flight test accelerometer measurements at  $\alpha = 20$  deg showing the Strouhal scaling of the dominant spectral peak.

#### Strouhal Number Matching

Figure 10 presents data from various sources for the frequency of the spectral peak near the vertical tail at a 20-deg angle of attack. The ordinate is the Strouhal number based on the freestream velocity and the mean aerodynamic chord. The relation between frequency and velocity is seen to be linear. Reference 3 mentions hot-wire tests performed near both a rigid vertical tail model as well as an aeroelastically scaled model in a low-speed wind tunnel. The model scale was 13%, and the tunnel dynamic pressure was  $384 \text{ N/m}^2$ . It was observed that the dominant frequency of the spectra varied with angle of attack, and the frequency of the dominant peak was plotted as a function of angle of attack. This provided additional data to study a Strouhal number correlation. Since freestream velocity was not given, it was approximated using sea-level standard pressure ( $1.013 \text{ N/m}^2$ ) and a static temperature of  $273.2 \text{ K}$  (St. Louis, Missouri, in November 1978–March 1979) to be  $24.35 \text{ m/s}$ . Reference 4 shows the acceleration spectrum at the top of the left vertical tail, measured during flight test of the full-scale aircraft. This spectrum exhibits a dominant frequency. The freestream conditions for this flight test had to be approximated, since only the dynamic pressure ( $11,395 \text{ N/m}^2$ ) was specified; these were taken to be Mach 0.6 at  $6096 \text{ m}$  ( $20,000 \text{ ft}$ ) standard pressure altitude based on the description of the flight test. A final data point for the correlation in Fig. 10 was taken using our  $\frac{1}{7}$ -scale model, at  $\alpha = 20$  deg and  $U_\infty = 12.19 \text{ m/s}$ . The data in Fig. 10 span 3 orders of magnitude in Reynolds number, and go from Mach 0.05 to Mach 0.6. The dynamic pressure ranges from  $32.08 \text{ N/m}^2$  to  $11,395 \text{ N/m}^2$ . Data from rigid models, elastic models and the full-scale vehicle are included. The Strouhal number averaged over all of the GT data (both  $\frac{1}{7}$  and  $\frac{1}{3}$  scale models) is 0.74; the flight test point gives 0.78, and the approximated McAir 13% model result gives 0.622. This provides strong evidence that in modeling the frequency of the strongest observed tail vibrations, Reynolds number and Mach number matching are not of primary importance. Of course these parameters are important for the modeling of other phenomena. The detailed flow over the panels of the vertical tail, for example, must depend on Reynolds number to some extent, and perhaps on local Mach number to a considerable extent.

The spectrum measured near and upstream of the vertical tail of the  $\frac{1}{7}$ -scale model is shown in Fig. 11. Clearly, the same phenomena are present as in the flowfield of the  $\frac{1}{3}$ -scale model. The hot-wire signal, monitored on an oscilloscope, showed that the fluctuations were intermittent occurrences, rather than a continuous periodic signal.

#### Strouhal Shedding: Distinction Between Tail Stalling and Wing Stalling

It is important to draw a distinction between this Strouhal number scaling and the previous investigations of Strouhal shedding on the F-15. Reference 3 discusses the possibility of periodic shedding of vorticity from the vertical tails themselves as a cause of the severe fluctuations. This possibility

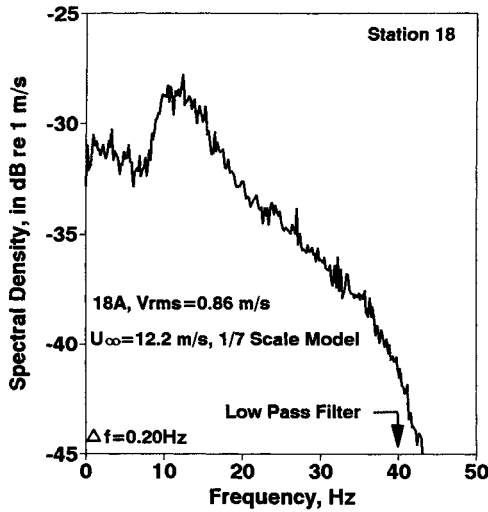


Fig. 11 Velocity spectrum upstream of the vertical tail of a  $\frac{1}{7}$ -scale model in the JJH tunnel at 12.19 m/s,  $\alpha = 20$  deg.

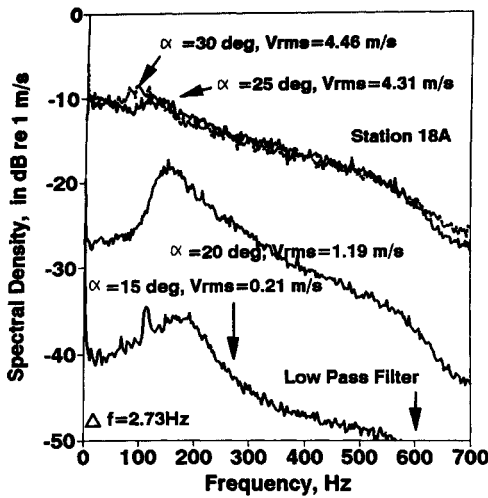


Fig. 12 Spectra of velocity fluctuations near the top of the vertical tail of the  $\frac{1}{7}$ -scale model for various angles of attack.

was discounted by considerations of geometry and by the fact that the buffeting did not occur during low- $\alpha$ , high-sideslip flight.<sup>3</sup> The present finding is not related to this. Here, the Strouhal number correlates the periodicity of the flowfield, beginning well upstream of the vertical tails, and enveloping the upper portions of the tails. On the other hand, the high instantaneous values of flow angularity upstream of the tail from the laser velocimeter data,<sup>1</sup> coupled with the visual observations of tuft dynamics,<sup>1</sup> suggest that stalling does occur intermittently on the tail surfaces, although there is no evidence that this leads to periodicity.

#### Variation of Dominant Frequency with Aircraft Angle of Attack

Figure 12 shows spectra at different angles of attack for the  $\frac{1}{7}$ -scale model, at station 18A at 30.48 m/s freestream velocity. Up to 10 deg, a weak spectral peak was seen at a low frequency. At 15 deg, there is already evidence of a sharp peak, along with a broader hump around 200 Hz. At 20 deg, the energy of this entire peak appears to be concentrated in the much narrower peak at 148 Hz, as seen before. Going to 25 deg, the spectrum is much broader. At 30 deg, multiple peaks appear.

Similar behavior has been observed in the buffeting pressure spectra near the vertical tails of the F/A-18 by Wentz<sup>5</sup> in water tunnel tests, and Zimmerman et al.<sup>6</sup> in wind tunnel and flight data. They also found that a different  $\alpha$ , the peaks in the buffet spectrum would move into the range of excitation

of different structural modes, resulting in a "tuning" of the vibration. These findings referred to fluctuations attributed to the bursting of the strong leading-edge vortex of that aircraft; no such vortex is present here.

Figure 13 summarizes the variation of dominant frequency with angle of attack. Even on a linear ordinate scale, there is some ambiguity in the choice of the dominant peak above 25 deg. Thus, Fig. 13 examines what would happen to the frequency of a given spectral feature as angle of attack increases. The frequency is seen to decrease. This phenomenon has precedents in the fluid dynamics literature. Thus, Ref. 7 shows periodicity in the wake of a two-dimensional wing at high  $\alpha$ , with a Strouhal number of 0.15 based on the projection of the chord normal to the freestream. As angle of attack increases, the projected chord would decrease, and thus, for a given Strouhal number, the frequency would decrease. The  $f^* \sin \alpha$  curve on Fig. 13, matched to the data at 20 deg, shows the variation seen here has some qualitative similarity, but is quantitatively quite different from the two-dimensional result.

#### Variation of Fluctuation Amplitude

Figure 14 plots the rms velocity at station 18A against the square of the freestream velocity. It is seen that the relation is fairly linear over the range from 6.096 to 30.48 m/s. The level of fluctuation increases with angle of attack, leveling off at about 25 deg, where the rms is of the order of 15% of the mean. Figure 15 shows the variation of the amplitude of the dominant peak of the velocity spectrum with freestream velocity. Again, this peak also rises in amplitude with freestream velocity and levels off.

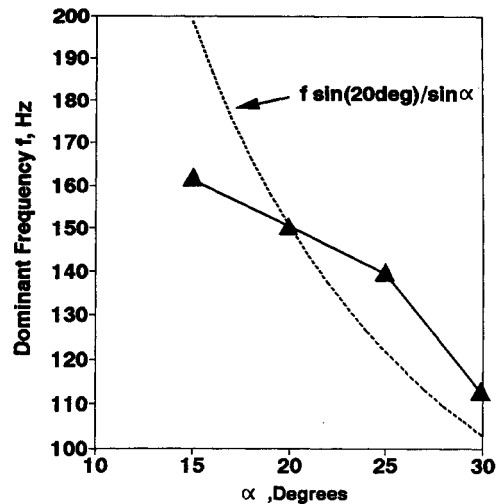


Fig. 13 Frequency of the dominant peak as a function of angle of attack, measured near the top of the vertical tail of the  $\frac{1}{7}$ -scale model at 30.48 m/s, compared with an  $(f^* \sin \alpha)$  variation.

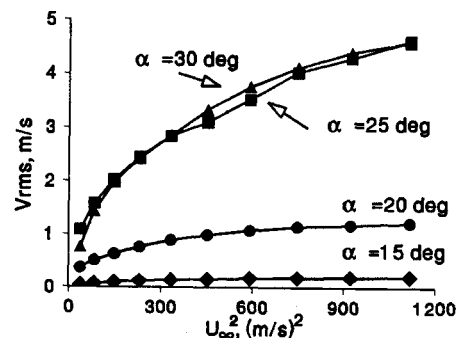


Fig. 14 Variation of the root-mean-square velocity fluctuation (with frequencies below 600 Hz), with the square of freestream velocity,  $\frac{1}{7}$ -scale model for several angles of attack.

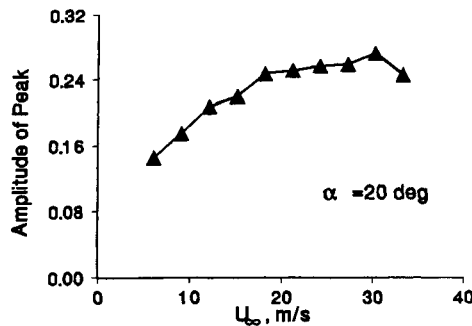


Fig. 15 Variation of the amplitude of the dominant spectral peak with freestream velocity:  $\frac{1}{2}$ -scale model at  $\alpha = 20$  deg.

### Conclusions

The frequency content of the fluctuating flowfield over scale models of the F-15 aircraft have been studied at high angles of attack using hot-film anemometry. The following conclusions are drawn:

- 1) Fluctuations upstream of the wing are mostly broadband, with high-frequency humps.
- 2) The spectra over the wing show the development of a narrow-band peak.
- 3) A dominant spectral peak occurs upstream, inboard and outboard of the top of the vertical tails.
- 4) The dominant frequency is linear with freestream velocity at a fixed angle of attack.
- 5) The frequency of the peak and the shape of the spectra change with aircraft angle of attack. For angles of attack above 30 deg, multiple peaks are observed.
- 6) At other portions of the vertical tail and elsewhere in the vortex flow over the aircraft the spectra show the broadband nature attributed to random turbulent flow.
- 7) For aircraft models of different size, tested at different velocities, the frequency of the dominant peak in the spectrum at the top of the vertical tail scales with Strouhal number.
- 8) The Strouhal number of the dominant frequency of fluctuation observed in model-scale tests of rigid vertical tails matches that of the peak of the acceleration spectrum mea-

sured in flight, at Mach 0.6 at the top of the full-scale aircraft vertical tail.

9) A spectral hump similar to that associated with the inlet vortex system appears between the vertical tails. This can cause fluctuating loads on the tail inner surfaces at frequencies approximately 3 times that of the outboard flow.

10) The spectral shapes are quite similar on both the inboard and outboard sides of the vertical tail; however, the level of fluctuations is much lower on the inboard side.

### Acknowledgments

This work was supported under Contract F09063-85-G-3104-0030 by the United States Air Force, WRALC. W. Phillips and Dave Curry are the Technical Monitors. The authors gratefully acknowledge the assistance of Jae-Soo Hyun, Visiting Scholar, in acquiring some of the LDV data, and of Scott Percival, undergraduate student in building the  $\frac{1}{2}$ -scale model of the F-15. Several valuable suggestions came from Howard M. McMahon.

### References

- <sup>1</sup>Komerath, N. M., Liou, S-G, Schwartz, R. J., and Kim, J. M., "Flow over a Twin-Tailed Aircraft at Angle of Attack, Part I: Spatial Characteristics," *Journal of Aircraft* (to be published).
- <sup>2</sup>Triplett, W. E., "Pressure Measurements on Twin Vertical Tails in Buffeting Flow," *Journal of Aircraft*, Vol. 20, No. 11, 1983, pp. 920-925.
- <sup>3</sup>Colvin, B. J., Mullans, R. E., Paul, R. J., and Roos, H. N., "F-15 Vertical Tail Vibration Investigations," McDonnell-Douglas Corporation Rept. A6114, McDonnell Aircraft Company, St. Louis, MO, Sept. 15, 1979.
- <sup>4</sup>Colvin, J., Spectra from L/H Vertical Tail Tip Pod Accelerometer, F-15A, A/C 71-0283, Flight 813, Run 6, 11/09/83, in "F-15 Vertical Stabilizer History," McDonnell Aircraft Co., St. Louis, MO, Jan. 18, 1989.
- <sup>5</sup>Wentz, W. H., "Vortex-Fin Interaction on a Fighter Aircraft," AIAA-87-2474, AIAA 5th Applied Aerodynamics Conf., Monterey, CA, Aug. 1987.
- <sup>6</sup>Zimmerman, N. H., Ferman, M. A., Yurkovich, R. N., and Gerstenkorn, G., "Prediction of Tail Buffet Loads for Design Applications," AIAA Paper 89-1378-CP, 1989.
- <sup>7</sup>Krzywoblocki, M. Z., "Investigation of the Wing-Wake Frequency with Application of the Strouhal Number," *Journal of the Aeronautical Sciences*, Vol. 12, Jan. 1945.